Biophysical Journal
Article

Biophysical Society

Mechanism of ArcLight derived GEVIs involves electrostatic interactions that can affect proton wires

Bok Eum Kang,[1] Lee Min Leong,[1,2] Yoonkyung Kim,[1] Kenichi Miyazaki,[3] William N. Ross,[3] and Bradley J. Baker[1,2,*]

[1]Brain Science Institute, Korea Institute of Science and Technology, Seongbuk-gu, Seoul, Republic of Korea; [2]Division of Bio-Medical Science and Technology, KIST School, Korea University of Science and Technology (UST), Seoul, Republic of Korea; and [3]Department of Physiology, New York Medical College, Valhalla, New York

ABSTRACT The genetically encoded voltage indicators ArcLight and its derivatives mediate voltage-dependent optical signals by intermolecular, electrostatic interactions between neighboring fluorescent proteins (FPs). A random mutagenesis event placed a negative charge on the exterior of the FP, resulting in a greater than 10-fold improvement of the voltage-dependent optical signal. Repositioning this negative charge on the exterior of the FP reversed the polarity of voltage-dependent optical signals, suggesting the presence of "hot spots" capable of interacting with the negative charge on a neighboring FP, thereby changing the fluorescent output. To explore the potential effect on the chromophore state, voltage-clamp fluorometry was performed with alternating excitation at 390 nm followed by excitation at 470 nm, resulting in several mutants exhibiting voltage-dependent, ratiometric optical signals of opposing polarities. However, the kinetics, voltage ranges, and optimal FP fusion sites were different depending on the wavelength of excitation. These results suggest that the FP has external, electrostatic pathways capable of quenching fluorescence that are wavelength specific. One mutation to the FP (E222H) showed a voltage-dependent increase in fluorescence when excited at 390 nm, indicating the ability to affect the proton wire from the protonated chromophore to the H222 position. ArcLight-derived sensors may therefore offer a novel way to map how conditions external to the β-can structure can affect the fluorescence of the chromophore and transiently affect those pathways via conformational changes mediated by manipulating membrane potential.

SIGNIFICANCE ArcLight-type genetically encoded voltage indicators send charge information outside of the FP to the internal chromophore enabling voltage induced conformational changes to affect fluorescence. These pathways are excitation wavelength specific, suggesting that different external positions affect the protonated and deprotonated states of the chromophore.

INTRODUCTION

Proton wires enable the long-range transfer of protons through a protein via a chain of hydrogen bonds (1,2). This chain of hydrogen bonds restricts the proton transfer along closely spaced oxygen, nitrogen, or sulfur atoms, allowing for the rapid transfer of charge. Fluorescent proteins (FPs) are an ideal model system for studying proton transfers because the protonation state of the chromophore as well as the hydrogen bond network near the chromophore affect the fluorescent properties of the protein (3–7). Here, we report evidence that the ArcLight family of genetically encoded voltage indicators (GEVIs) modulate their fluorescence via intermolecular electrostatic interactions that can modulate proton wires in FPs.

GEVIs convert transients in membrane potential into changes in fluorescence intensity, allowing simultaneous measurements at multiple locations from subcellular regions like the endoplasmic reticulum of a neuron (8) to population signals in neuronal circuits (9,10). GEVIs can be mutated to change the speed of the voltage response (11,12), the size of the optical signal (13–15), the voltage range of the optical signal (16), or the photophysical properties of the probe (17–19). Further improvement of GEVIs would benefit from a better understanding of the mechanism(s) mediating the voltage-induced fluorescence change.

The GEVI, ArcLight, was the result of a serendipitous mutation to the FP domain (14). This unintended mutation introduced a negative charge to the exterior of the β-can structure of the FP resulting in a 15-fold improvement in

Submitted October 6, 2020, and accepted for publication March 10, 2021.

*Correspondence: bradley.baker19@gmail.com

Editor: Meyer Jackson.

https://doi.org/10.1016/j.bpj.2021.03.009

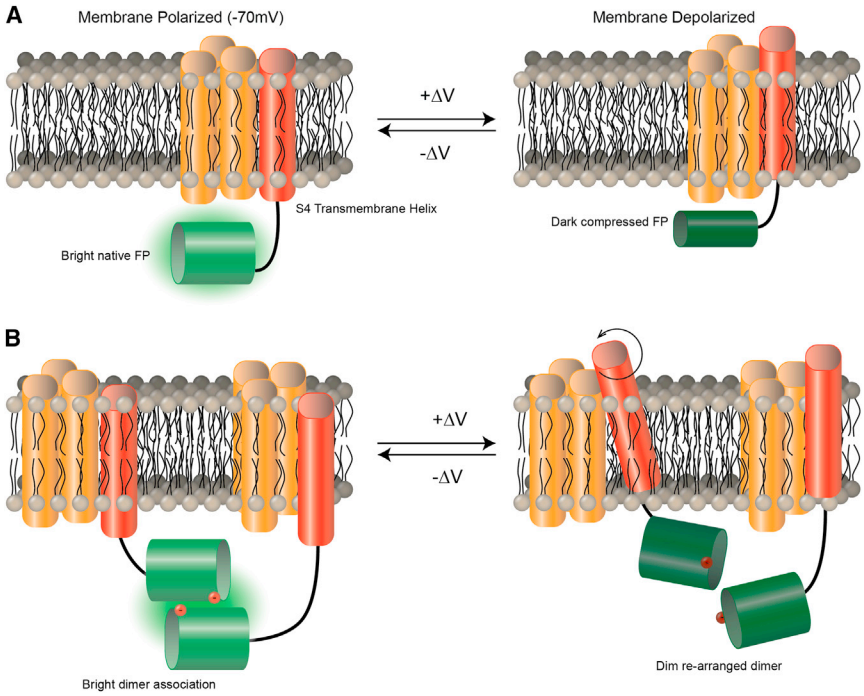

FIGURE 1 Two models for voltage-mediated fluorescence change of ArcLight-type GEVIs. (*A*) The compression model modified from Simine et al. (21) suggesting a depolarization of the plasma membrane potential ($+\Delta V$) distorts the β-can structure, causing a decrease in fluorescence. (*B*) The dimerization model suggesting that the repositioning of a negative charge in relationship to a neighboring chromophore causes a change in fluorescence in response to voltage transients.

the voltage-dependent optical signal. ArcLight consists of an FP in the cytoplasm fused to a classical four-transmembrane, voltage-sensing domain (VSD) (20) that resides in the plasma membrane, enabling the GEVI to optically report changes in membrane potential (Fig. 1). How alterations to the membrane potential mediate changes in fluorescence intensities or why the addition of a negative charge to the protein outside of the voltage field in the cytoplasmic domain of the GEVI resulted in a dramatic improvement in the optical signal have been difficult to explain.

One potential mechanism suggested that physical compression of the FP domain against the plasma membrane caused the dimming of fluorescence for ArcLight in response to depolarization of the plasma membrane (Fig. 1 *A*; (21)). While that report demonstrated that compression of the β-can structure could alter the environment of the chromophore for ArcLight, the compression mechanism does not explain the requirement of an external negative charge on the FP at position 227 (A227D; numbering throughout refers to the amino acid position in the FP) (14,17), the increase in fluorescence during hyperpolarization of the plasma membrane, or the apparent requirement for the FP to be pH sensitive (17).

An alternate model describing the mechanism of ArcLight's voltage-dependent optical response involves an intermolecular interaction of ArcLight via the FP domain. Introduction of mutations that favor the monomeric form of the FP in ArcLight reduced the voltage-dependent optical signal by at least 70% (22), suggesting the hypothesis that conformational changes in the VSD move the external negative charge along the β-can of a neighboring FP, altering the environment of the chromophore (Fig. 1 *B*).

In this report we present evidence that suggests the negative charge on the exterior of the β-can mediates voltage-dependent optical signals via electrostatic interactions between neighboring probes. Repositioning the negative charge along the outside of the β-barrel structure of the FP resulted in the polarity of the optical response being reversed when the membrane potential was manipulated. The position of the external negative charge determined whether the fluorescence became brighter or dimmer in response to depolarization of the plasma membrane. This result suggests an electrostatic interaction between associated FP domains mediating the voltage-dependent optical signal. Because the FP for ArcLight is pH-sensitive, these results support the scenario that the position of the negative charge in relation to a neighboring chromophore simulates a pH-like effect on the fluorescence of the GEVI with the speed of the response now dependent upon the movement of the VSD responding to changes in membrane potential. This electrostatic interaction of ArcLight-type GEVIs offers the potential to improve the magnitude of the voltage-dependent fluorescent response as well as provide insights into how environmental conditions at the exterior of the β-can structure can affect the internal chromophore of the FP.

MATERIALS AND METHODS

Subcloning

The Triple Mutant (TM) construct is described in Piao et al. (11). Point mutations were made through directed mutagenesis through PCR. Oligonucleotides were synthesized (Cosmo Genetech, Seoul, South Korea) and PCR was performed to make the target insert (Bio-Rad Laboratories, Hercules,

CA). Inserts were cloned into pcDNA3.1 Hygro + vector using restriction enzymes (New England Biolabs, Ipswich, MA). Completed constructs were verified by sequencing (Cosmo Genetech, Seoul, South Korea; Bionics, Seoul, South Korea).

GEVI expression

HEK 293 cells were maintained in DMEM supplemented with 10% v/v FBS (Gibco Laboratories, Gaithersburg, MD) at 37°C (5% CO_2) and were seeded onto poly-L-lysine (Sigma-Aldrich, St. Louis, MO) coated #0 glass coverslips (Ted Pella, Redding, CA). Transfections were performed at a cell confluency of ~70% with lipofectamine 2000 (Invitrogen, Carlsbad, CA). Cells were usually tested 14 h posttransfection.

Patch-clamp fluorometry

Patch-clamp experiments were performed on an inverted microscope (Olympus, Shinjuku, Tokyo, Japan). The chamber that held the seeded glass coverslips had a constant flow of bath solution heated to 35°C. The bath solution contained 150 mM NaCl, 4 mM KCl, 2 mM $CaCl_2$, 1 mM $MgCl_2$, and 5 mM D-glucose and was buffered with 5 mM HEPES at pH 7.4 with NaOH. A 75 W xenon arc lamp (Cairn Energy, Edinburgh, UK) provided the light for the excitation of fluorophores. Two filter cubes were used, one composed of an excitation filter at 472 nm (FF02-472/30-25), a dichroic mirror at 495 nm (FF495-Di03-25x36), and a long pass emission filter at 496 nm (FF01-496/LP-25). The second filter cube used the same setup except for the excitation filter, which was optimized for 390 nm light (FF01-386/26-25) (Semrock, Rochester, NY). The pipette electrodes were pulled from capillary tubing (World Precision Instruments, Sarasota, FL) by a pipette puller (Sutter Instruments, Novato, CA) to a resistance of 3–5 MΩ. The pipette solution contained 120 mM K-aspartate, 4 mM NaCl, 4 mM $MgCl_2$, 1 mM $CaCl_2$, 10 mM EGTA, 3 mM Na_2ATP, and was buffered with 5 mM HEPES at pH 7.2. The HEK cells were clamped and their membrane potential manipulated using an HEKA EPC10 amplifier (HEKA Elektronik, Westfield, MA). An Optem Zoom System demagnifier (Qioptiq, St Asaph Denbighshire, UK) connected the fast imaging camera to the c-mount output of the microscope. The demagnified image was projected onto the 80 × 80 CCD chip of the NeuroCCD camera which was used to image fluorescence at frame rate of 1 KHz (RedShirt Imaging, Decatur, GA). The entire system was mounted on an air table to reduce the vibrational noise.

Data analysis

Data acquisition was controlled through the Neuroplex program (RedShirt Imaging), which was also the platform from which we exported the ascii data for further analysis using the Origin software package (Origin Labs, Northampton, MA). Traces were averages of four trials and off-line filtering with a 100 Hz Butterworth filter unless otherwise indicated.

RESULTS

The position of the negative charge on the surface of the FP determines the polarity of the voltage-dependent optical signal

The A227D mutation to the FP of ArcLight that was responsible for a 15-fold improvement in the voltage-dependent optical signal resides on the 11th β-strand with the side chain external to the β-can structure (14). The role of this external negative charge was examined by performing an aspartic acid mutagenesis scan along the external residues of the 11th β-strand (Fig. 2 *A*) of an ArcLight-derived GEVI TM, which has a longer linker segment of amino acids between the VSD and the FP and exhibits faster kinetics (11).

Mutant constructs consisting of a single external negative charge at different positions along the 11th β-strand were expressed in HEK 293 cells while the plasma membrane potential was manipulated via whole-cell voltage clamp (Fig. 2 *A*). When the aspartic acid residue was at the original 227 position in the FP (A227D), the optical signal got brighter upon hyperpolarization of the plasma membrane and dimmer during depolarization (Fig. 2 *B*). When the negative charge was moved to the 225 position (A227/T225D, the next residue on the β-strand with its side chain external to the β-can structure), the voltage response was quite different. The hyperpolarizing signal was nearly eliminated whereas the depolarizing signal consisted of at least two components with opposing polarities; there was a rapid, initial increase in fluorescence followed by a slower decrease in fluorescence. Repositioning the negative charge to the next external residue (A227/T225/F223D) resulted in the complete reversal of the polarity for the optical signal compared with the original A227D construct. The hyperpolarization response got dimmer, whereas the depolarization response got brighter. Moving the negative charge further up the β-strand to positions L221D or V219D showed similar patterns to the F223D construct albeit reduced in signal size. These results demonstrate that the position of the negative charge determines the polarity of the fluorescent response of the GEVI in response to membrane potential changes.

The position of the external negative charge also affected the polarity of the voltage-dependent optical signal when TM was excited at 390 nm instead of at 470 nm (Fig. 2 *B*). As mentioned in the introduction, the protonation state of the chromophore for wild-type GFP determines the excitation wavelength. The protonated, neutral state is excited at 390 nm, whereas the deprotonated, anionic state is excited at 470 nm (3–5,25). TM also uses the FP, Super Ecliptic pHlorin (SEpH), which is pH-sensitive and contains the S65T mutation to reduce the 390 nm excitation peak (26,27). Despite the S65T mutation in the FP, the aspartic acid scan constructs were capable of yielding a voltage-dependent optical signal when excited at 390 nm that also reversed orientation depending on the position of the external negative charge (Fig. 2 *B*).

Introduction of the T65S mutation to the FP domain inverts the polarity of the optical response for TM but not ArcLight

The observation that the position of the external negative charge in the FP domain determined the polarity of the voltage-dependent optical signal suggested the possibility that the negative charge was affecting the protonation state of the chromophore. The ability of TM to exhibit a voltage-dependent optical signal that changed polarities

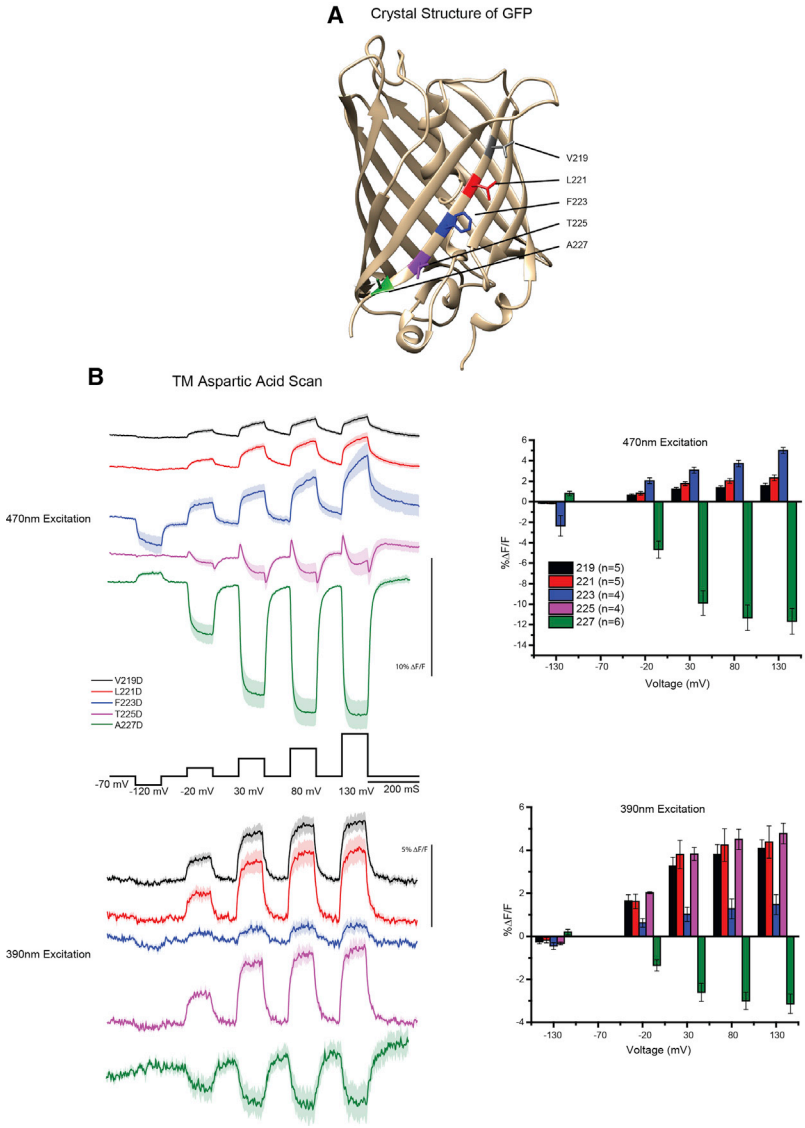

FIGURE 2 The position of the external, negative charge along the 11th β-strand of the fluorescent protein determines the polarity of the voltage-dependent optical signal. (*A*) The crystal structure of GFP (PDB: 1EMA) from Ormö et al. (23) showing the position of the external residues along the 11th β-strand. The structure was annotated using the Chimera program (24). (*B*) Optical traces from HEK cells expressing a GEVI with the negative charge at the A227 position (A227D, *green*), the T225 position (T225D, *purple*), the F223 position (F223D, *blue*), the L221 position (L221D, *red*), or the V219 position (V219D, *black*). Upper traces are from experiments using 470 nm excitation light. Lower traces are from experiments using 390 nm excitation light. The command voltage of the whole-cell voltage clamp protocol is shown in black (holding potential was −70 mV). All traces were filtered offline with a Butterworth low pass 100 Hz filter. The solid line in the traces represents the average of at least four cells which is also shown in the bar graphs on the right. The shaded areas in the traces represent the standard error of the mean (error bars in bar graphs).

when excited at 390 nm was surprising because ArcLight was previously shown to give a voltage-dependent optical signal that decreased in fluorescence intensity when the protonated form of the chromophore was excited; although in that report, 400 nm light was used for excitation rather than the 390 nm light used in these experiments (18).

To better understand the different behavior of these GEVIs when excited at 390 nm, we compared the ArcLight and TM constructs having the T65 version of the FP, SEpH (28), to the reverse-engineered constructs with improved 390 nm excitation (the Ecliptic pHlorin version of the FP) (26), designated epArcLight T65S and epTM T65S (Fig. 3). HEK 293 cells expressing these constructs were imaged under voltage clamp fluorometry with alternate trials consisting of excitation at 390 nm followed by excitation at 470 nm on the same cell.

ArcLight (T65) gave small, but distinct voltage-dependent signals with peculiar properties when excited with 390 nm light (Fig. 3 *A*). For a 50 mV depolarization of the plasma membrane, the fluorescence dimmed slightly. For a 100 mV depolarization, there was a fast component that got brighter followed by a slower component that got dimmer. Stronger depolarizations of the plasma membrane with a 150 mV or a 200 mV step exhibited a fast, transient component that got brighter and a slower, persistent component that also increased the fluorescence of the probe when compared with the fluorescence at the holding potential of −70 mV. Introduction of the T65S mutation into the FP (epArcLight) reduced the complexity of the voltage-dependent optical signal when excited at 390 nm but did not exhibit an increase in fluorescence upon depolarization of the plasma membrane when excited at 390 nm.

TM (T65) exhibited a different response than ArcLight when excited at 390 nm (Fig. 3 *B*). Regardless of excitation wavelength, the fluorescence of TM (T65) was reduced during depolarization steps. However, introduction of the T65S

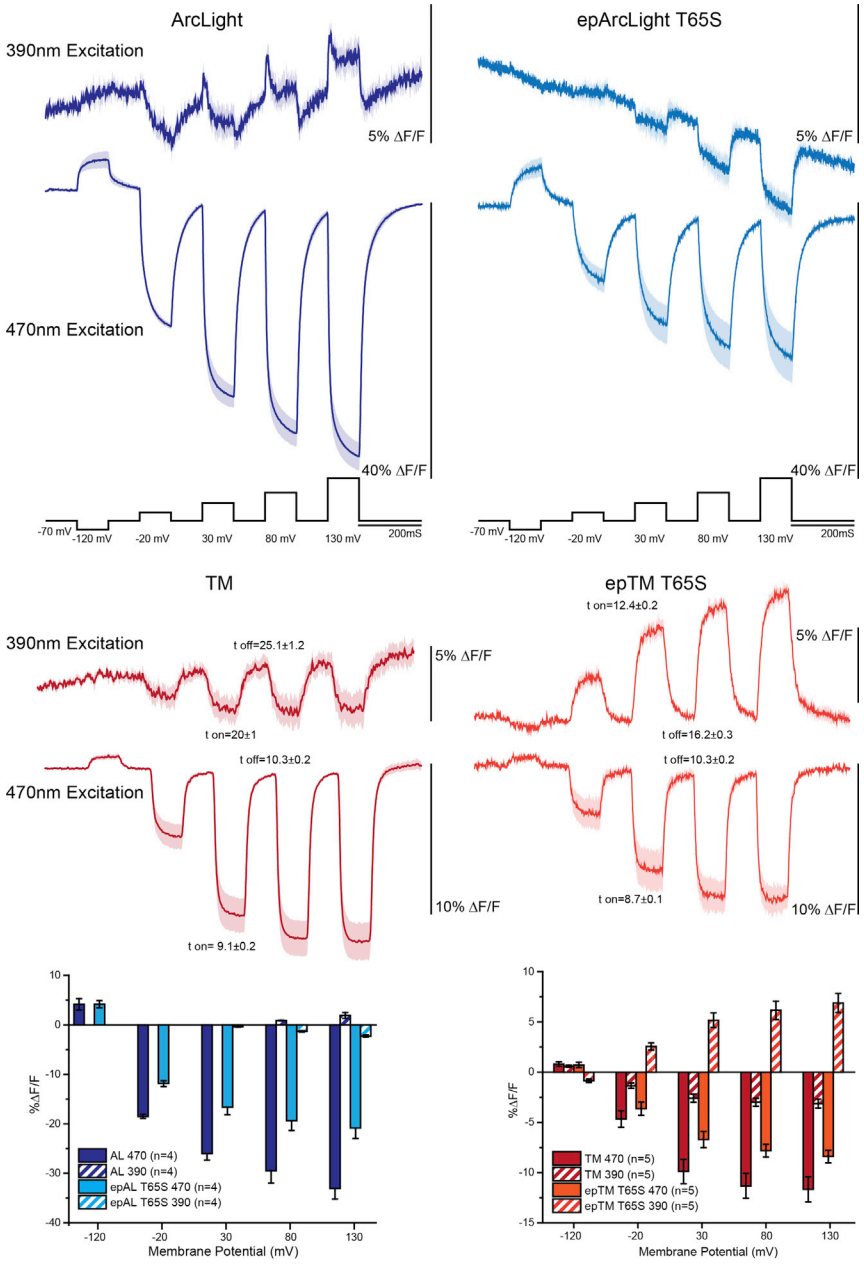

FIGURE 3 Excitation state dependence of anti-correlated fluorescence change for the GEVI, epTM T65S. Traces depict voltage-dependent optical signals from HEK cells expressing ArcLight-T65 (*dark blue*), epArcLight-T65S (*light blue*), TM-T65 (*dark red*), or epTM-T65S (*light red*). The command voltage is shown in black. For each construct, optical signals were recorded using either 390 nm excitation light (*top traces*) or 470 nm excitation light (*bottom traces*). Shaded regions of the traces and error bars in the graphs are both standard error of the mean. All traces were filtered offline with a low pass Butterworth 100 Hz filter. τ values are given for the 100 mV depolarization step for both TM and epTM. The solid line in the traces represents the average of at least four cells which is also shown in the bar graphs below. The shaded areas in the traces represent the standard error of the mean (error bars in bar graphs).

mutation (epTM) inverted the polarity of the voltage-dependent optical signal when excited at 390 nm. Initially we believed the inverted polarity for the epTM T65S mutant was the result of a shift in the protonation state of the chromophore. The voltage-induced conformational change during depolarization steps favored the protonated state of the chromophore causing the fluorescence to increase when excited at 390 nm and to decrease when excited at 470 nm. However, closer inspection of the optical responses for both excitation wavelengths revealed that the kinetics and voltage ranges of the optical signals for the two excitation wavelengths were different. The τ of the response, which is the time constant required to achieve 63% of the maximal response for epTM T65S at 390 nm for a 100 mV depolarization step, was 12.4 $\pm$ 0.2 ms, whereas the τ of the response at 470 nm was 8.7 $\pm$ 0.1 ms. Upon returning to the holding potential, the speed of the optical response for both wavelengths were again different, exhibiting a τ of 16.2 $\pm$ 0.3 ms when excited at 390 nm compared with a τ of 10.3 $\pm$ 0.2 ms when excited with 470 nm light (Fig. 3).

The voltage range was also different depending on the wavelength of excitation. The signal size for the 390 nm recording continued to increase even for the 200 mV depolarization step, whereas the 470 nm recording plateaued at the 150 mV step, suggesting different mechanisms for different excitation wavelengths. Indeed, the mechanism

of voltage-dependent fluorescence change may be chromophore-state specific because the voltage-dependent optical signals for both GEVIs containing the Ecliptic pHlorin version of the FP were reduced when excited at 470 nm (Fig. 3) compared with the original versions of the GEVIs.

Even though the mechanism of the voltage-induced optical signal did not involve a simple transition in the protonation state of the chromophore, the ability of the GEVIs to yield signals when excited at different wavelengths offered a potential for the development of ratio-metric probes capable of quantitating membrane potential. We therefore attempted to optimize the voltage-dependent signal for both the 390 and 470 nm wavelengths using the T65S version of the FP.

The length of the linker between the VSD and the FP affects the polarity of the optical signal when excited at 390 nm but not 470 nm

A general method for improving the optical signal of GEVIs is to vary the number of amino acids between the VSD and the FP (11,19,29–31). We employed this strategy in the hope of generating a ratiometric probe with a dynamic response sufficient for in vivo recordings. GEVIs were constructed containing the Ecliptic version of the FP because epTM T65S exhibited an inverse correlation dependent upon excitation wavelength during depolarization of the plasma membrane (Fig. 3). The linker segments between the VSD and the FP domain ranged from 4 to 24 amino acids (Fig. 4). HEK cells expressing constructs of varying linker lengths were voltage clamped and imaged with alternating trials of 390 and 470 nm excitation light.

Surprisingly, the optimal linker length differed depending on the excitation wavelength. The optimal linker length for the 470 nm excitation signal was around seven to eight amino acids in length, whereas a longer linker of 15 amino acids yielded the best voltage-dependent signal for 390 nm excitation. Interestingly, the polarity of the voltage-dependent optical signal during 390 nm excitation inverted as the linker length was shortened. The fluorescence decreased upon depolarization of the plasma membrane when the linker length was less than six amino acids yet the fluorescence increased for linker lengths greater than eight. This explains why little to no signal was seen previously for ArcLight upon 390 nm excitation. The linker length for ArcLight is around eight to nine amino acids depending on the version being used which are poor locations for the FP during 390 nm excitation recordings.

Mutations to the E222 position can rescue the 390 nm voltage-dependent optical signal

The different optimal linker lengths for the voltage-dependent signal when excited at 390 nm compared with 470 nm suggested that the negative charge was affecting the protonated state of the chromophore differently than the anionic state. Different linker lengths could alter the positioning of the negative charge on the exterior of the FP in relationship to the neighboring chromophore upon movement of the VSD domain in response to voltages changes at the plasma membrane. The optimal position of the negative charge when excited at 390 nm was different than when excited at 470 nm. The hotspot responding to the voltage-induced movement of the negative charge may be wavelength dependent.

The fluorescence of SEpH is highly sensitive to pH (26,28), indicating that a pathway or pathways exist for the proton concentration outside of the β-can structure to affect the fluorescence of the internal chromophore. Proteins have been shown to contain proton wires that allow for the rapid transfer of protons to different positions in the protein (6,7,32). For instance, excitation of wild-type GFP with 390 nm light results in an excited-state proton transfer involving the protonated form of the chromophore (5,7,25,33). The E222 position has been postulated as the terminal proton acceptor in this transfer process (6,7,34,35). In the presence of S65, the E222 side chain is coordinated to create a proton wire from Y66 (chromophore) to E222 via at least one water molecule and S205 (Fig. 5). The S65T mutation alters the coordination of E222 thereby disrupting the proton wire. E222 is also near the position of the external negative charge that reverses the polarity of the voltage-dependent optical signal (Fig. 2). The proton wire in the protonated state of the chromophore for wild-type GFP has also been reported to contain low-barrier hydrogen bonds (7), which describes a hydrogen weakly bonded to both the hydrogen donor and hydrogen acceptor simultaneously (37). Bringing an external charge near E222 could then potentially alter this charge network and thereby affect the fluorescent properties of the chromophore. We therefore tested four E222 mutations that varied in charge or polarity (E222Q, E222D, E222K, and E222H) in the presence of the S65 FP (390 nm excitation peak) or the T65 FP (470 nm excitation peak).

The E222Q mutants gave modest voltage-dependent optical signals when excited at 470 nm light (Fig. 5). However, when excited with 390 nm light, neither the E222Q/65S nor the E222Q/65T constructs gave a voltage-dependent signal. This is consistent with the previous finding that the E222Q mutation destabilizes the protonated form of the chromophore (35).

The E222D/65T mutant response was very similar to the original GEVI, TM. The voltage-dependent optical signal was larger when excited at 470 nm than when excited at 390 nm (Fig. 4). This was also the case for the E222/65T construct (Fig. 2). The E222D mutation in the presence of the Ecliptic S65 version of the FP exhibited a nearly 8-fold reduction in the voltage-dependent signal when

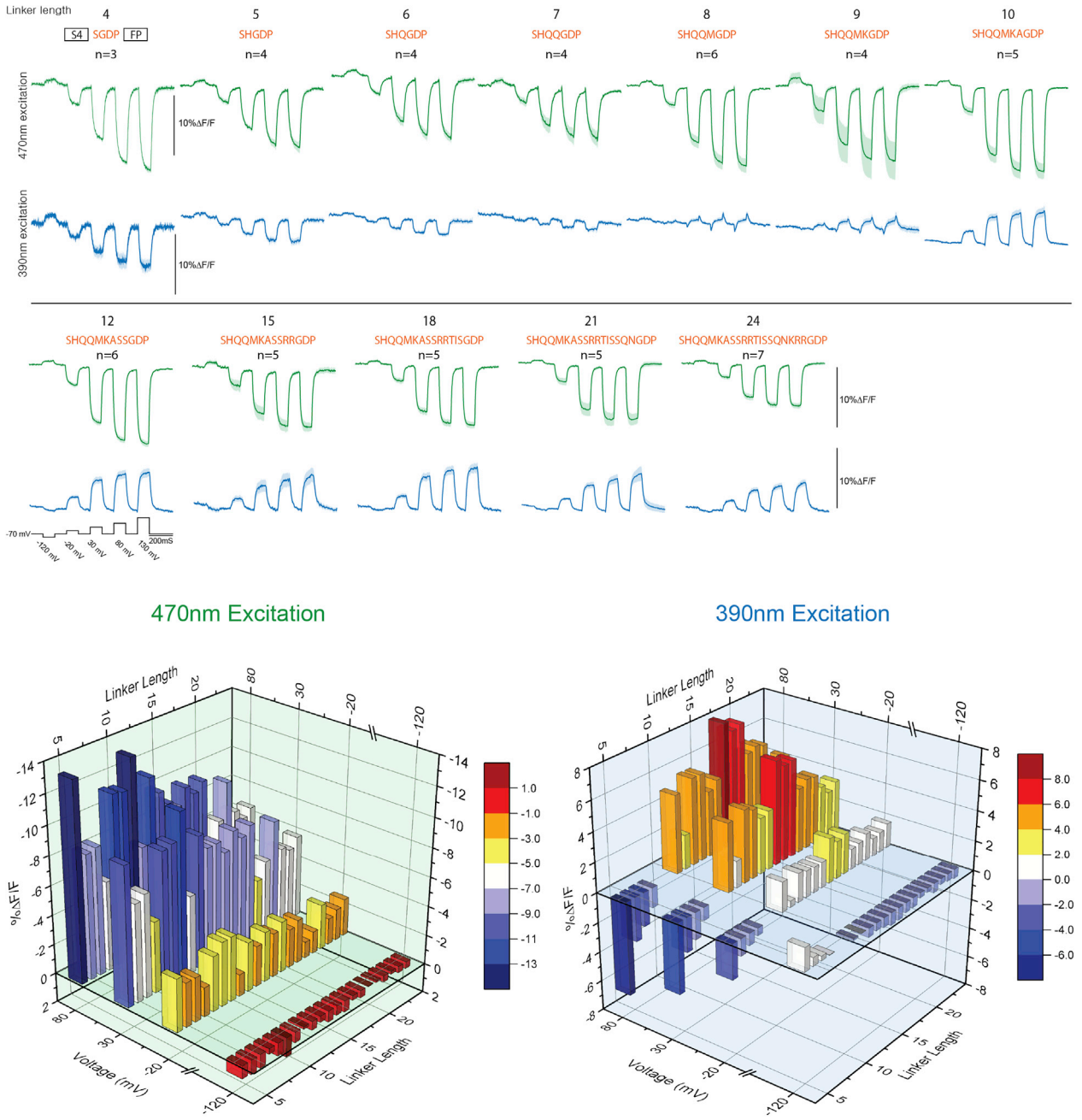

FIGURE 4 Linker length affects the voltage-dependent optical signal differently when excited at 390 nm (*blue traces*) than at 470 nm (*green traces*). Optical traces from HEK cells expressing the GEVI, epTM T65S, with varying linker lengths from four amino acids to 24 amino acids between the VSD (*box* labeled VSD) and the fluorescent protein (*box* labeled FP). The linker protein sequence in red is based on the *Ciona* phosphatase gene. The GDP sequence is from the Bam HI cloning site, which is also included as part of the linker sequence. Numbers above indicate total number of amino acids between the VSD and the FP. The 8 and 9 linker length constructs excited at 390 nm were omitted from the bar graphs below because of the complex nature of those signals. The command voltage steps are shown in black under the 12 linker trace. All traces were filtered offline with a low pass Butterworth 100 Hz filter. The solid line in the traces represents the average of at least three cells. The shaded areas in the traces represent the standard error of the mean.

excited at 470 nm (Fig. 5). Interpretation of the signal for E222D/65T with 390 nm excitation with a small yet short-lived increase in fluorescence in response to depolarization of the plasma membrane suggests a very transient effect induced by the movement of the external negative charge.

Reversing the charge with the E222K mutations did not destroy the voltage-dependent signal when excited at 470 nm light regardless of whether there was a threonine or serine residing at position 65 (Fig. 5). Excitation at 390 nm yielded very little, if any, fluorescence for both

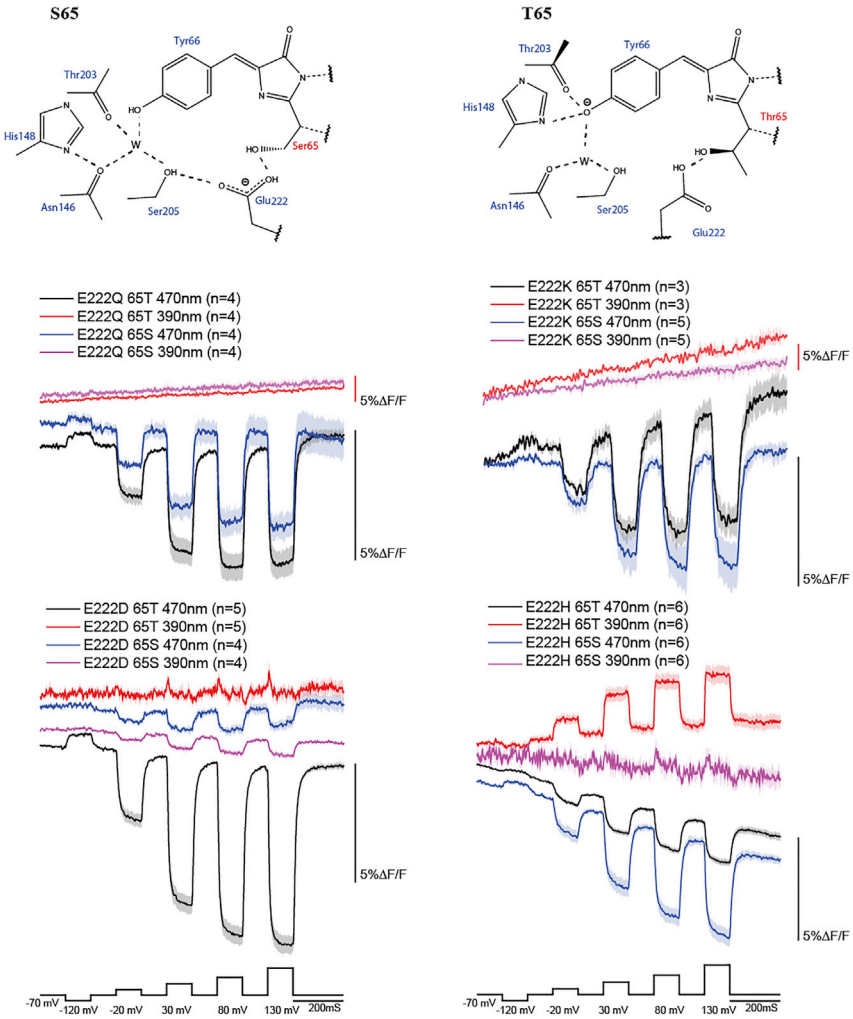

FIGURE 5 Manipulating the proton wire from the chromophore to E222 via voltage transients of the plasma membrane. Top left is the chemical structure of the protonated chromophore with an intact proton wire from Y66 to E222 via a water molecule (W) and the hydroxyl group of S205 in the presence of S65. Top right is the chemical structure of the anionic chromophore with a disrupted proton wire due to an altered orientation of E222 in the presence of T65 (reproduced with permission from Armengol et al. (36), published by the PCCP Owner Societies). Below are the voltage-dependent optical traces of E222 mutants with the SEpH (T65) or the Ecliptic (S65) version of the FP expressed in HEK cells. The voltage command pulse protocol is shown at the bottom of both columns in black. Shaded regions in the traces are standard errors of the mean. All traces were filtered offline with a low pass Butterworth 100 Hz filter. The solid line in the traces represents the average of at least three cells. The shaded areas in the traces represent the standard error of the mean.

E222K/65T or E222K/65S constructs. As a result, no voltage-dependent signal was observed.

Like the other E222 mutations, the E222H/T65 and E222H/S65 mutants exhibited a voltage-dependent signal when excited at 470 nm (Fig. 5). However, the E222H/S65 construct is the only S65 mutant with a larger voltage-dependent signal than the T65 version when excited at 470 nm. Surprisingly, the E222H/65T mutant also yielded an optical signal in the opposite direction when excited at 390 nm. In contrast, the E222H/65S construct yielded a barely detectable change in fluorescence when excited at 390 nm, suggesting that the E222H mutant, upon a voltage-induced conformational change, can reestablish the proton wire from the protonated chromophore to H222 and thereby rescue the fluorescence of the protein when excited at 390 nm but only in the presence of T65 not S65.

DISCUSSION

The mechanism of voltage-mediated fluorescence change for ArcLight-type GEVIs appears to involve an electrostatic interaction between FP domains of two adjacent probes. In contrast to the structural rearrangements that might be caused by the compression of the FP onto the plasma membrane (21), the interaction of neighboring FPs creates an environment that can be altered by voltage-induced conformational changes. This FP dimerization model accounts for the effect of the A227D mutation placing a negative charge on the exterior of the β-can structure, the inverted polarity of the voltage-dependent optical signal upon hyperpolarization of the plasma membrane, and the effects of varying the linker length between the VSD and the cytosolic FP.

The challenge now is to determine with which amino acids on the neighboring FP the A227D residue is interacting. SEpH is a pH-sensitive FP that gets dimmer upon acidification of the surrounding environment (26,27,38). Initial attempts to use SEpH as the fluorescent reporter in GEVIs resulted in probes yielding a very modest change in fluorescence (1% ΔF/F/100 mV) upon depolarization of the plasma membrane (14), indicating that pH-sensitivity of the FP alone is not sufficient to explain the large

optical signal seen for ArcLight. Fortunately, a spontaneous mutagenesis event that introduced a negatively charged amino acid on the exterior of the FP domain (A227D) resulted in a 15-fold larger voltage-dependent optical signal.

In this report, we have shown that the position of this external charge matters. Moving the negative charge along the exterior of the β-strand resulted in the reversal of the polarity of the voltage-dependent optical signal (Fig. 2), suggesting that the electrostatic environment of the FP has been altered by the movement of the VSD in response to voltage. When the negative charge is at the 227 position, depolarization results in a voltage-dependent reduction of the fluorescence. When the negative charge is at positions 219, 221, or 223, the fluorescence of the GEVI gets brighter upon depolarization of the plasma membrane. This may indicate that depolarization of the plasma membrane results in the FP experiencing a more acidic environment when the negative charge is at position 227 relative to the initial environment during the holding potential. Because the lack of a negative charge on the FP results in small, voltage-dependent optical changes, we conclude that A227D is responsible for the generation of this novel environment. In agreement, introduction of monomeric favoring mutations to the FP domain of ArcLight reduced the voltage-dependent fluorescence change by over 70% (22).

One way to affect the fluorescence of the FP is to modulate the protonation state of the chromophore. GFP has two excitation peaks. The protonated state of the chromophore is excited at 390 nm, whereas the anionic chromophore is excited at 470 nm (Fig. 5). If the movement of the external negative charge in response to voltage affected the protonation state of a neighboring chromophore, the result would be an anticorrelated optical signal dependent upon the wavelength of excitation. Protonation of the chromophore would reduce the 470 nm excitation signal while simultaneously increasing the 390 nm excitation signal and vice versa. However, although the polarity of the voltage-dependent optical signals were anticorrelated depending on the wavelength of excitation, the speeds and voltage ranges of those optical responses were different (Fig. 3). Further evidence suggesting that the mechanism of fluorescence change is not a simple transition in chromophore protonation state comes from the fact that the linker length separating the FP from the VSD could reverse the polarity of the voltage-dependent signal during excitation with 390 nm light but not with 470 nm excitation light (Fig. 4). For constructs consisting of a linker shorter than seven amino acids, the fluorescence decreases upon depolarization of the plasma membrane regardless of whether the excitation wavelength is 390 or 470 nm.

Having ruled out a direct effect on the protonation state of the chromophore as the only cause of fluorescence change, the mechanism of the voltage-dependent fluorescence change may involve transient changes to proton wires affecting amino acids neighboring the chromophore. One indication this may be the case can be seen in the E222 mutations. E222 is the proton acceptor for the excited state proton transfer upon excitation at 390 nm (4,6,7,25). Changing E222 to aspartic acid, lysine, or glutamine abolished or greatly diminished the voltage-dependent optical signal when excited with 390 nm light. However, the E222H mutant yielded an increase in fluorescence upon depolarization of the plasma membrane when excited at 390 nm, suggesting a potential rescue of the proton transfer pathway for the protonated chromophore but only when the S65T mutation is present (Fig. 5). Hopefully, molecular modeling simulations will reveal if this rescue is via the same proton pathway or the generation of a new one.

SEpH is capable of transmitting an environmental change in pH from the exterior of the β-can to the chromophore in the interior. There must be a route for the external environmental conditions to affect the chromophore and may be true for other FPs. Indeed, a recently developed red fluorescent protein, stagRFP, was rationally designed by neutralizing an external acidic residue on the β-barrel (39). This led to a reduction in the blinking to the dark state, which improved the fluorescence of the FP. In addition, molecular dynamic simulations revealed the presence of many novel proton wires potentially capable of transferring protons from the chromophore to the bulk solution (6). These multiple pathways linking the interior of the FP to the exterior environment may explain the biphasic nature of some of the optical traces as asynchronous interaction of the A227D residue with those pathways would depend upon the movement of the FP.

Our current hypothesis, based on the evidence presented here, is that the movement of the VSD alters fluorescence by repositioning a negative charge near the pH-sensing region of a neighboring FP. This would also explain why different linker lengths alter the voltage-dependent signal in different ways, as the pathway the negative charge of the A227D residue transverses upon movement of the VSD would be different when the linker length is changed. Fig. 4 shows that the optimal linker length for the voltage-dependent signal for 390 nm excitation recordings is indeed different from that at 470 nm.

ArcLight-type GEVIs offer the exciting possibility of differentiating/mapping these pathways by transiently altering electrostatic interactions between FP domains. The pathways could be controlled by manipulating the voltage of the plasma membrane. Indeed, by combining molecular modeling and structural data, it may be possible to map the movement of the FP in conjunction with the movement of the VSD, further improving the development of

GEVIs as well as revealing how protons are moving through the FP.

AUTHOR CONTRIBUTIONS

B.E.K. designed and performed experiments, analyzed data, and assisted in the writing of the manuscript. L.M.L. assisted with experiments involving variable linker lengths. Y.K. assisted with experiments positioning the negative charge along the exterior of the FP. K.M. assisted with the ratiometric experiments and data analysis. W.N.R. assisted with the ratiometric experiments and data analysis. B.J.B. designed experiments, assisted with data analysis, and helped write the manuscript.

ACKNOWLEDGMENTS

We thank Lawrence Cohen for critical review of the manuscript.

Research reported in this publication was supported by the National Institute of Neurological Disorders and Stroke of the National Institutes of Health under Award Number U01NS099691. K.M. and W.N.R. were supported by National Institutes of Health grant R01NS099122. The content is solely the responsibility of the authors and does not necessarily represent the official views of the National Institutes of Health. This study was also funded by the Korea Institute of Science and Technology grant 2E30963. Molecular graphics and analyses performed with UCSF Chimera, developed by the Resource for Biocomputing, Visualization, and Informatics at the University of California, San Francisco, with support from NIH P41-GM103311.

REFERENCES

1. Cukierman, S. 2003. The transfer of protons in water wires inside proteins. *Front Biosci.* 8:s1118–s1139.
2. Nagle, J. F., and H. J. Morowitz. 1978. Molecular mechanisms for proton transport in membranes. *Proc. Natl. Acad. Sci. USA.* 75:298–302.
3. Chattoraj, M., B. A. King, …, S. G. Boxer. 1996. Ultra-fast excited state dynamics in green fluorescent protein: multiple states and proton transfer. *Proc. Natl. Acad. Sci. USA.* 93:8362–8367.
4. Agmon, N. 2005. Elementary steps in excited-state proton transfer. *J. Phys. Chem. A.* 109:13–35.
5. Heim, R., D. C. Prasher, and R. Y. Tsien. 1994. Wavelength mutations and posttranslational autoxidation of green fluorescent protein. *Proc. Natl. Acad. Sci. USA.* 91:12501–12504.
6. Shinobu, A., and N. Agmon. 2017. Proton wire dynamics in the green fluorescent protein. *J. Chem. Theory Comput.* 13:353–369.
7. Di Donato, M., L. J. G. W. van Wilderen, …, M. L. Groot. 2011. Proton transfer events in GFP. *Phys. Chem. Chem. Phys.* 13:16295–16305.
8. Sepehri Rad, M., L. B. Cohen, …, B. J. Baker. 2018. Monitoring voltage fluctuations of intracellular membranes. *Sci. Rep.* 8:6911.
9. Nakajima, R., and B. J. Baker. 2018. Mapping of excitatory and inhibitory postsynaptic potentials of neuronal populations in hippocampal slices using the GEVI, ArcLight. *J. Phys. D Appl. Phys.* 51:504003.
10. Storace, D. A., and L. B. Cohen. 2017. Measuring the olfactory bulb input-output transformation reveals a contribution to the perception of odorant concentration invariance. *Nat. Commun.* 8:81.
11. Piao, H. H., D. Rajakumar, …, B. J. Baker. 2015. Combinatorial mutagenesis of the voltage-sensing domain enables the optical resolution of action potentials firing at 60 Hz by a genetically encoded fluorescent sensor of membrane potential. *J. Neurosci.* 35:372–385.
12. Kralj, J. M., A. D. Douglass, …, A. E. Cohen. 2011. Optical recording of action potentials in mammalian neurons using a microbial rhodopsin. *Nat. Methods.* 9:90–95.
13. Lee, S., T. Geiller, …, B. J. Baker. 2017. Improving a genetically encoded voltage indicator by modifying the cytoplasmic charge composition. *Sci. Rep.* 7:8286.
14. Jin, L., Z. Han, …, V. A. Pieribone. 2012. Single action potentials and subthreshold electrical events imaged in neurons with a fluorescent protein voltage probe. *Neuron.* 75:779–785.
15. Chamberland, S., H. H. Yang, …, F. St-Pierre. 2017. Fast two-photon imaging of subcellular voltage dynamics in neuronal tissue with genetically encoded indicators. *eLife.* 6:e25690.
16. Jung, A., D. Rajakumar, …, B. J. Baker. 2017. Modulating the voltage-sensitivity of a genetically encoded voltage indicator. *Exp. Neurobiol.* 26:241–251.
17. Han, Z., L. Jin, …, V. A. Pieribone. 2014. Mechanistic studies of the genetically encoded fluorescent protein voltage probe ArcLight. *PLoS One.* 9:e113873.
18. Platisa, J., G. Vasan, …, V. A. Pieribone. 2017. Directed evolution of key residues in fluorescent protein inverses the polarity of voltage sensitivity in the genetically encoded indicator ArcLight. *ACS Chem. Neurosci.* 8:513–523.
19. Yi, B., B. E. Kang, …, B. J. Baker. 2018. A dimeric fluorescent protein yields a bright, red-shifted GEVI capable of population signals in brain slice. *Sci. Rep.* 8:15199.
20. Murata, Y., H. Iwasaki, …, Y. Okamura. 2005. Phosphoinositide phosphatase activity coupled to an intrinsic voltage sensor. *Nature.* 435:1239–1243.
21. Simine, L., H. Lammert, …, P. J. Rossky. 2018. Fluorescent proteins detect host structural rearrangements via electrostatic mechanism. *J. Am. Chem. Soc.* 140:1203–1206.
22. Kang, B. E., and B. J. Baker. 2016. Pado, a fluorescent protein with proton channel activity can optically monitor membrane potential, intracellular pH, and map gap junctions. *Sci. Rep.* 6:23865.
23. Ormö, M., A. B. Cubitt, …, S. J. Remington. 1996. Crystal structure of the Aequorea victoria green fluorescent protein. *Science.* 273:1392–1395.
24. Pettersen, E. F., T. D. Goddard, …, T. E. Ferrin. 2004. UCSF Chimera–a visualization system for exploratory research and analysis. *J. Comput. Chem.* 25:1605–1612.
25. Agmon, N. 2005. Proton pathways in green fluorescence protein. *Biophys. J.* 88:2452–2461.
26. Miesenböck, G., D. A. De Angelis, and J. E. Rothman. 1998. Visualizing secretion and synaptic transmission with pH-sensitive green fluorescent proteins. *Nature.* 394:192–195.
27. Ng, M., R. D. Roorda, …, G. Miesenböck. 2002. Transmission of olfactory information between three populations of neurons in the antennal lobe of the fly. *Neuron.* 36:463–474.
28. Sankaranarayanan, S., D. De Angelis, …, T. A. Ryan. 2000. The use of pHluorins for optical measurements of presynaptic activity. *Biophys. J.* 79:2199–2208.
29. Dimitrov, D., Y. He, …, T. Knöpfel. 2007. Engineering and characterization of an enhanced fluorescent protein voltage sensor. *PLoS One.* 2:e440.
30. Jung, A., J. E. Garcia, …, B. J. Baker. 2015. Linker length and fusion site composition improve the optical signal of genetically encoded fluorescent voltage sensors. *Neurophotonics.* 2:021012.
31. Han, Z., L. Jin, …, V. A. Pieribone. 2013. Fluorescent protein voltage probes derived from ArcLight that respond to membrane voltage changes with fast kinetics. *PLoS One.* 8:e81295.
32. Pomès, R., and B. Roux. 1996. Structure and dynamics of a proton wire: a theoretical study of H+ translocation along the single-file water chain in the gramicidin A channel. *Biophys. J.* 71:19–39.
33. Brejc, K., T. K. Sixma, …, S. J. Remington. 1997. Structural basis for dual excitation and photoisomerization of the Aequorea victoria green fluorescent protein. *Proc. Natl. Acad. Sci. USA.* 94:2306–2311.
34. Lill, M. A., and V. Helms. 2002. Proton shuttle in green fluorescent protein studied by dynamic simulations. *Proc. Natl. Acad. Sci. USA.* 99:2778–2781.

35. Jung, G., J. Wiehler, and A. Zumbusch. 2005. The photophysics of green fluorescent protein: influence of the key amino acids at positions 65, 203, and 222. *Biophys. J.* 88:1932–1947.

36. Armengol, P., L. Spörkel, …, J. M. Lluch. 2018. Ultrafast action chemistry in slow motion: atomistic description of the excitation and fluorescence processes in an archetypal fluorescent protein. *Phys. Chem. Chem. Phys.* 20:11067–11080.

37. Cleland, W. W. 1992. Low-barrier hydrogen bonds and low fractionation factor bases in enzymatic reactions. *Biochemistry.* 31:317–319.

38. Shen, Y., M. Rosendale, …, D. Perrais. 2014. pHuji, a pH-sensitive red fluorescent protein for imaging of exo- and endocytosis. *J. Cell Biol.* 207:419–432.

39. Mo, G. C. H., C. Posner, …, J. Zhang. 2020. A rationally enhanced red fluorescent protein expands the utility of FRET biosensors. *Nat. Commun.* 11:1848.